



# Neutrino Flavor Conversion Shapes the Rate of Failed Core-collapse Supernovae

Mariam Gogilashvili <sup>1,\*</sup> and Irene Tamborra <sup>1,†</sup>

<sup>1</sup>*Niels Bohr International Academy and DARK, Niels Bohr Institute,  
University of Copenhagen, Blegdamsvej 17, 2100, Copenhagen, Denmark*

The relative rate of neutron stars and black holes produced by the collapse of massive stars is highly uncertain. We simulate the stellar collapse of 195 progenitors with masses between  $9 M_{\odot}$  and  $120 M_{\odot}$ , incorporating a schematic treatment of neutrino flavor conversion. We find that flavor transformation reshapes the explodability of massive stars—especially in the  $16\text{--}30 M_{\odot}$  mass range—and modifies the compact remnant mass distribution. Our findings identify neutrino flavor conversion as a fundamental ingredient in predicting neutron star and black hole populations, while naturally easing the red-supergiant and the supernova-rate problems, as well as reconciling theoretical expectations with the low-mass tail of the observed neutron star mass distribution.

**Introduction.**— When a star with mass  $M \gtrsim 8 M_{\odot}$  exhausts its nuclear fuel, its iron core undergoes gravitational collapse. If neutrino heating successfully revives the stalled shock wave, the star explodes as a core-collapse supernova (CCSN), leading to the formation of a neutron star [1, 2]. Otherwise, if the star fails to explode, it collapses, forming a black hole [3–5]. Determining which massive stars explode as CCSNe and which collapse into black holes remains a major unsolved problem in astrophysics, with direct implications for the birth rates and mass distributions of neutron stars and black holes, nucleosynthesis, and stellar feedback.

It was initially believed that black hole formation could occur only for progenitor stars with mass exceeding  $40 M_{\odot}$  [6], affecting the distribution of neutron star and black hole masses [6–9]. However, recent work, based on spherically symmetric simulations of the stellar collapse, has jeopardized such understanding, revealing that the CCSN explodability is non-monotonic with the progenitor mass, and black holes can originate from CCSN progenitors with mass as low as  $13 M_{\odot}$  [10–14].

On the observational side, growing evidence suggests that massive stars may undergo failed explosions, leading to optically dark or faint transients [15–21]. These findings suggest that about 5–50% of all collapses fail to produce a visible explosion, consistent with theoretical expectations [10–14, 22] and the preliminary exclusion limits on the fraction of failed explosions from the diffuse supernova neutrino background [23–26]. Failed CCSNe may contribute to address the red supergiant problem (i.e., the absence of red supergiant progenitors in the mass range  $16\text{--}30 M_{\odot}$  among identified Type IIP supernova progenitors) [27, 28] as well as the CCSN rate problem (i.e., the fact that the observed cosmic CCSN rate falls systematically below the rate inferred from the cosmic star formation rate) [29]. In addition, radio pulsar and X-ray binary observations provide evidence for a neutron star mass distribution in the range  $1.2\text{--}2.1 M_{\odot}$ , with a dearth of black holes below  $5 M_{\odot}$  [30–34]. These constraints have recently been complemented by the detection of gravitational waves from compact binary mergers [35–37]. Accounting for these observational constraints simultane-

ously challenges theoretical CCSN models [8, 12, 14, 38], suggesting that key physics, governing the explosion mechanism and determining which progenitors fail to explode, is yet to be established.

The CCSN explosion mechanism is driven by neutrinos. The latter are weakly interacting elementary particles that carry away about 99% of the gravitational binding energy [ $\mathcal{O}(10^{53})$  erg] of the proto-neutron star formed during the core collapse. Electron neutrinos and antineutrinos mediate the energy transfer behind the stalled shock through charged-current interactions [1]; whether their energy deposition is sufficient to revive the shock ultimately determines the fate of the collapse.

Despite its crucial role in driving the fate of the explosion, neutrino physics in CCSNe is not fully understood. In particular, state-of-the-art multi-dimensional hydrodynamic simulations of CCSNe do not account for the fact that neutrinos can change their flavor while propagating in the CCSN core (see, e.g., Refs. [39–45] for an overview). The assumption that neutrino flavor conversion (FC) could be neglected in the modeling of the explosion mechanism was justified by the understanding that FC would have a negligible effect behind the shock [46]. However, recent insights into the physics of neutrino self-interaction question this picture as they show that FC can take place even in the surroundings of the proto-neutron star [47–53]. If neutrino FC occurs in the CCSN core, it can affect the neutrino-driven delayed explosion mechanism, as suggested by preliminary work accounting for FC in CCSN simulations using schematic approaches [54–60].

In this *Letter*, for the first time, we explore whether FC affects the rate of failed CCSNe and the properties of the compact remnants. For this purpose, we build on Ref. [60], that employs the instantaneous flavor equilibration of (anti)neutrinos from Ref. [54] in 1D+ CCSN simulations performed with GR1D [61–63]. We investigate the impact of FC on the fate of the CCSN explosion using a set of 195 progenitors with solar metallicity from Ref. [12] with masses between  $9 M_{\odot}$  and  $120 M_{\odot}$ .

Our results suggest that FC increases the fraction of failed explosions, especially in the  $16\text{--}30 M_{\odot}$  mass range,

potentially helping to address the supernova rate problem. Moreover, when FC occurs near the stalled shock, it accelerates shock revival, yielding less massive neutron stars, in better agreement with the observed mass distribution.

**Model Setup.**—We model the stellar collapse using the open-source, spherically symmetric code GR1D [61, 62], which evolves general-relativistic hydrodynamics coupled to energy-dependent neutrino transport. As detailed in Ref. [60], our simulations employ a radial grid with 850 zones, resolving the innermost 20 km with uniform spacing and increasing logarithmically at larger radii. The hydrodynamics is solved using a finite-volume approach with second-order Runge–Kutta time integration, capturing both the collapse of the iron core and the post-bounce evolution. Neutrino transport is treated with an energy-dependent moment formalism using M1 closure for three species ( $\nu_e$ ,  $\bar{\nu}_e$ , and  $\nu_x = \bar{\nu}_x$ , with  $x = \mu$  or  $\tau$ ) over 18 energy bins. Neutrino–matter interactions are modeled using tabulated rates from NuLib [62]. To account for the effects of neutrino-driven convection and turbulence, we employ the Supernova Turbulence in Reduced-dimensionality (STIR) model [63, 64], with the turbulence strength set by the dimensionless parameter  $\alpha_{\text{MLT}} = 1.51$ .

Flavor conversion is taken into account using the parametric scheme proposed in Refs. [54, 65], which instantaneously leads to flavor equipartition, while conserving electron lepton number as well as the number and momentum of (anti)neutrinos for each energy bin. We apply the equipartition scheme to each energy bin shortly after bounce ( $t = 0.02$  s) in regions where the matter density is below a threshold baryon density  $\rho_c$ , varied between  $10^{13}$  and  $10^9$  g/cm<sup>3</sup>, i.e., spanning the radial region between the neutrinosphere and the stalled shock. By modifying the relative spectra of electron neutrinos, electron antineutrinos, and heavy-lepton neutrinos, FC affects charged-current heating and cooling in the region behind the shock, thereby altering the conditions for shock revival [54, 55, 60].

We simulate 195 progenitors from Ref. [12], spanning zero-age main-sequence (ZAMS) masses from  $9 M_\odot$  through  $120 M_\odot$ . This selection allows us to capture the diversity of pre-collapse cores, from low-mass stars with steep density gradients to more massive stars with extended, loosely bound envelopes. All CCSN models are simulated using the Steiner, Fischer, and Hempel (SFHo) equation of state [66]. Each progenitor is evolved from the onset of collapse through 1–3 s after core bounce.

To characterize the explodability potential of CCSNe (cf., e.g., Refs. [10–12, 67] for dedicated work in this direction), we use the progenitor compactness parameter [4]:  $\xi_M = (M/M_\odot)/[R(M)/1000 \text{ km}]$ , where  $R(M)$  is the radial coordinate enclosing a mass  $M$ . The compactness of our models is evaluated at  $M = 2.5 M_\odot$  just prior to collapse and is displayed in the top panel of Fig. 1.

**Fraction of Failed Supernovae.**—Figure 1 presents our results on the explodability landscape for 195 progen-

TABLE I. Fraction of the failed explosions for models without and with FC instantaneously triggered below the baryon density  $\rho_c$ . We list the fraction of our models that fails to explode ( $f_{\text{fail}}$ ) as well as the fraction of failed explosions weighted by the Salpeter IMF ( $f_{\text{Salp}}$ ).

$\rho_c$ [g/cm <sup>3</sup> ]	$f_{\text{fail}}$	$f_{\text{Salp}}$
No FC	25.6%	27.0%
$10^9$	50.8%	47.6%
$10^{10}$	77.4%	61.9%
$10^{11}$	93.3%	73.9%
$10^{13}$	96.4%	88.3%

itors with masses between  $9 M_\odot$  and  $120 M_\odot$ , simulated for five scenarios: without FC (No FC) and with FC imposed below the critical densities  $\rho_c = 10^9, 10^{10}, 10^{11}$ , and  $10^{13}$  g/cm<sup>3</sup>, from top to bottom, respectively. We assume that core collapse leads to a successful explosion (green bars) if the shock radius exceeds 1000 km, otherwise a failed supernova occurs (black bars).

Overall, we see that FC increases the fraction of failed explosions, especially in the 16–30  $M_\odot$  mass range. Figure 1 also suggest that the fraction of failed collapses increases with increasing  $\rho_c$ . Hence, the deeper inside the proto-neutron star flavor equilibration is achieved, the greater the suppression of shock revival. This trend reflects the overall tendency of FC in redistributing energy from electron-flavor neutrinos to heavy-flavor neutrinos, with a consequent decrease of the efficiency of neutrino energy deposition [60].

Without FC, 25.6% of our CCSN models fail to explode, in agreement with the existing literature based on spherically symmetric CCSN simulations [4, 10–12, 14]. If we account for the distribution of CCSN progenitors according to the Salpeter initial mass function (IMF) [68], the fraction of failed explosions is 27% in the absence of FC. This fraction is consistent with observational constraints [15–21]. When FC is taken into account, the IMF-weighted fraction of failed explosions increases, ranging from 47.6% for  $\rho_c = 10^9$  g/cm<sup>3</sup> to 88.3% for  $\rho_c = 10^{13}$  g/cm<sup>3</sup>, as summarized in Table I. Note that the IMF proposed in Ref. [69] leads to similar results (not shown here).

The changes induced by FC in the intermediate ZAMS mass range may contribute to alleviate the red supergiant problem [27, 28] as well as the supernova rate problem [29]. However, for  $\rho_c = 10^{11}$  and  $10^{13}$  g/cm<sup>3</sup>, the IMF-weighted fractions of failed collapses are 73.9% and 88.3%, seemingly in tension with observational constraints. These quantitative findings should be interpreted with caution. To compute the exact fraction of failed collapses, FC should be incorporated in CCSN simulations dynamically, accounting for the temporal evolution and spatial extent of FC. To this purpose, advanced multi-dimensional sub-grid models of FC—cf., e.g., Refs. [54, 65, 70–78] for recent efforts in this direction—should be embedded in

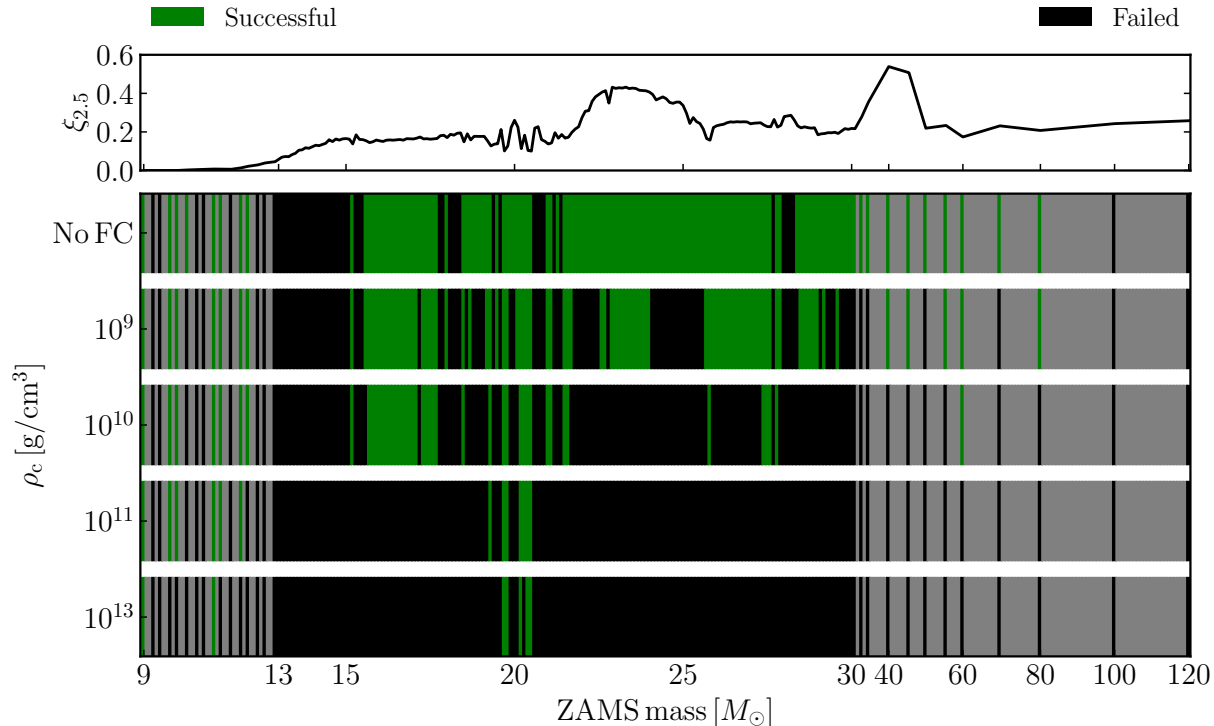


FIG. 1. Islands of explodability for CCSNe. *Top panel:* Pre-supernova core compactness ( $\xi_{2.5}$ ) as a function of the ZAMS mass showing the correlation between progenitor structure and CCSN explodability. *Bottom panel:* Islands of explodability as functions of the ZAMS mass. Each horizontal band displays successful (green) or failed (black) CCSN explosions; the gray bars denote progenitors that are not simulated. The top row represents the reference case without FC. From the second to the bottom row, respectively, FC is triggered below a critical baryon density:  $\rho_c = 10^9, 10^{10}, 10^{11}$ , and  $10^{13}$   $\text{g/cm}^3$ . Failed explosions are favored when FC is taken into account, especially in the 16–30  $M_{\odot}$  mass range.

CCSN simulations dynamically. Such subgrid models build on the understanding of FC coming from kinetic simulations of neutrino transport (currently still under development; see, e.g., Refs. [51, 79–85]). Moreover, our CCSN models do not account for proto-neutron star convection. However, FC triggered at high  $\rho_c$  is expected to boost convection in the hot proto-neutron star [86], with a consequent potential enhancement of neutrino heating. In addition, we model the CCSN population employing the SFHo nuclear equation of state, however, the impact of FC on the fate of the explosion may be quantitatively affected if other nuclear equations of state were to be considered [58, 60].

In the absence of FC, our CCSN progenitors [12] predict a large fraction of failed explosions in the range between 13  $M_{\odot}$  and 16  $M_{\odot}$ . Since low- and intermediate-mass progenitors are the most abundant according to the IMF, they drive the overall rate of failed explosions. It should be noted, however, that the predicted explodability landscape is sensitive to the choice of the progenitor set as well as the details of the physics implemented in the CCSN hydrodynamic simulation: different stellar evolution models

(e.g. Refs. [87, 88]) and different neutrino-driven explosion treatments (e.g. Refs. [4, 11, 38, 89, 90]) yield different distributions of failed and successful collapses, including in the 13–16  $M_{\odot}$  mass range. Furthermore, all progenitor models used in the literature on the topic are one dimensional, assuming spherical symmetry in the pre-collapse stellar structure. Three-dimensional CCSN simulations suggest that multidimensional effects in the progenitor (such as convective shell burning perturbations and asymmetries) can significantly alter the shock revival and thus the CCSN explodability [91, 92].

**Compact Remnant Properties.**—Flavor conversion also contributes to define the mass of the compact remnant, as shown in Fig. 2. The latter represents the baryonic mass ( $M_f$ ) enclosed within the energy- and flavor-averaged neutrinosphere radius, evaluated at  $t = 1$  s post-bounce or at the latest available time step for simulations that did not reach this time. For successful explosions (top panel of Fig. 2), FC leads to remnants more compact than those obtained when FC is not taken into account (colored vs. black points). Triggering earlier and more energetic shock revival, FC is responsible for less efficient

matter accretion onto the proto-neutron star, resulting in systematically lower  $M_f$ . The impact of FC on  $M_f$  becomes more pronounced at lower  $\rho_c$ , since the revival of the shock is more efficient [60].

For successful explosions,  $M_f$  spans the range between  $1.2 M_\odot$  and  $1.9 M_\odot$ . Hence, after accounting for the baryonic to gravitational mass correction, FC is responsible for gravitational masses that agree better with the bulk of the observed neutron star population, peaking around  $1.2\text{--}1.4 M_\odot$  [31, 32, 34], compared to the systematically higher neutron star masses obtained without FC. The lower gravitational mass obtained with FC thus eases the tension between CCSN theory and the observed low-mass end of the neutron star population [93].

For failed explosions (bottom panel of Fig. 2),  $M_f$  tends to be larger in the presence of FC, as the absence of shock revival allows for accretion onto the proto-neutron star to continue up to  $t = 1$  s post-bounce (or until black hole formation, if the latter occurs earlier). This effect is most pronounced for FC triggered at higher  $\rho_c$ , where shock revival is significantly delayed or suppressed, sustaining accretion for longer. Nevertheless, the effective change in the baryonic mass of the compact remnant induced by FC seems to be less prominent than for the case of successful explosions. Note, however, that  $M_f$  should not be interpreted as the final black hole mass; the latter could be substantially larger because of fallback accretion of the stellar envelope, if black hole formation occurs at  $t \gtrsim 1$  s.

**Conclusions.**—We investigate, for the first time, the impact of FC on the explodability of 195 CCSN progenitors with masses between  $9 M_\odot$  and  $120 M_\odot$  using 1D+hydrodynamic simulations. Our results show that FC has a profound impact on the CCSN explodability. In fact, overall, FC tends to reduce the net energy deposition behind the stalled shock, systematically favoring failed explosions.

We trigger FC instantaneously below a critical baryon density ( $\rho_c$ ), imposing flavor equipartition while conserving the electron lepton number as well as the number and momentum of neutrinos for each energy bin. As  $\rho_c$  increases, the fraction of failed explosions is larger due to more efficient neutrino cooling [60]. Importantly, the models with mass in the  $16\text{--}30 M_\odot$  range are particularly sensitive to FC, with a large number of otherwise successful explosions being converted into failures when FC is taken into account. The changes induced by FC in this mass range may help alleviate the red supergiant problem [27, 28] as well as the supernova rate problem [29]. We stress that the relative increase of failed explosions when FC is taken into account is robust with respect to our reference CCSN progenitor population that does not account for FC. However, our fraction of failed collapses is expected to be sensitive to the details of the simulation as well as our schematic treatment of FC.

The mass of the compact remnant left behind successful

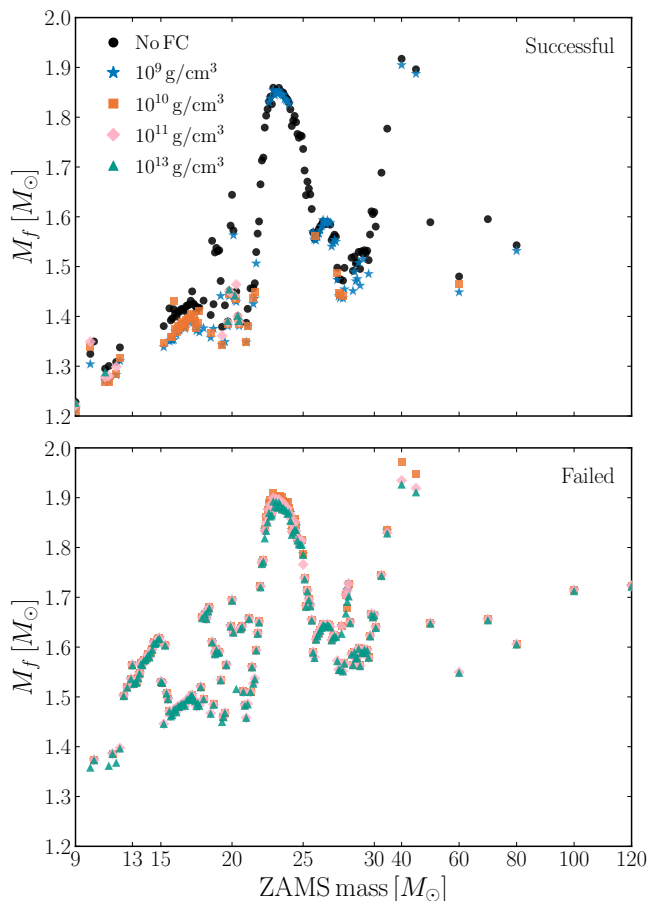


FIG. 2. Baryonic mass of the compact remnant evaluated at  $t = 1$  s post-bounce (or at the latest time step, if the black hole forms earlier) as a function of ZAMS mass. The final mass of the remnant is shown for the cases without FC (black circles) and with FC triggered below  $\rho_c = 10^9$  (blue stars),  $10^{10}$  (orange squares),  $10^{11}$  (pink diamonds), and  $10^{13}$   $\text{g}/\text{cm}^3$  (teal triangles). The progenitors that successfully explode (fail to explode) are represented in the upper (lower) panel. For successful explosions, the compact remnant mass is systematically smaller when FC is taken into account. Vice versa, when FC suppresses or prevents shock revival, leading to black hole formation, the remnant mass tends to be slightly larger (black and blue symbols are underneath the orange ones).

explosions is also affected by FC. We find systematically lower proto-neutron star masses in the CCSN models that account for FC, reflecting earlier shock revival and reduced post-bounce accretion. Our findings imply that FC should be taken into account in theoretical forecasts of the neutron star mass distribution, as gravitational-wave, X-ray and pulsar-timing observations establish a larger sample of neutron star masses [30–34, 94].

Neutrino FC is a key ingredient in modeling the birth rates and mass distributions of black holes and neutron stars. Advances in our understanding of the microphysics determining the collapse of massive stars are especially

needed, as a growing number of multi-messenger observations challenges our understanding of the physics driving the latest stages of the life of massive stars.

**Acknowledgments.**— We thank Luca Boccioli, Hans-Thomas Janka and Evan P. O’Connor for insightful discussions. This project has received support from the European Union (ERC, ANET, Project No. 101087058) and the Villum Foundation (Project No. 13164). Views and opinions expressed are those of the authors only and do not necessarily reflect those of the European Union or the European Research Council. Neither the European Union nor the granting authority can be held responsible for them. We used the Tycho supercomputer hosted at the SCIENCE HPC center at the University of Copenhagen to perform the numerical simulations presented in this work.

---

\* [mariam.gogilashvili@nbi.ku.dk](mailto:mariam.gogilashvili@nbi.ku.dk)

† [tamborra@nbi.ku.dk](mailto:tamborra@nbi.ku.dk)

- [1] H. A. Bethe and J. R. Wilson, Revival of a stalled supernova shock by neutrino heating, *Astrophys. J.* **295**, 14 (1985).
- [2] A. Burrows and J. M. Lattimer, The Birth of Neutron Stars, *Astrophys. J.* **307**, 178 (1986).
- [3] T. Fischer, S. C. Whitehouse, A. Mezzacappa, F. K. Thielemann, and M. Liebendörfer, The neutrino signal from protoneutron star accretion and black hole formation, *Astron. Astrophys.* **499**, 1 (2009), [arXiv:0809.5129](https://arxiv.org/abs/0809.5129) [[astro-ph](#)].
- [4] E. O’Connor and C. D. Ott, Black Hole Formation in Failing Core-Collapse Supernovae, *Astrophys. J.* **730**, 70 (2011), [arXiv:1010.5550](https://arxiv.org/abs/1010.5550) [[astro-ph.HE](#)].
- [5] A. Burrows, T. Wang, and D. Vartanyan, Channels of Stellar-mass Black Hole Formation, *Astrophys. J.* **987**, 164 (2025), [arXiv:2412.07831](https://arxiv.org/abs/2412.07831) [[astro-ph.SR](#)].
- [6] C. L. Fryer, Mass limits for black hole formation, *Astrophys. J.* **522**, 413 (1999), [arXiv:astro-ph/9902315](https://arxiv.org/abs/astro-ph/9902315).
- [7] K. Belczynski, G. Wiktorowicz, C. Fryer, D. Holz, and V. Kalogera, Missing Black Holes Unveil The Supernova Explosion Mechanism, *Astrophys. J.* **757**, 91 (2012), [arXiv:1110.1635](https://arxiv.org/abs/1110.1635) [[astro-ph.GA](#)].
- [8] C. L. Fryer, K. Belczynski, G. Wiktorowicz, M. Dominik, V. Kalogera, and D. E. Holz, Compact Remnant Mass Function: Dependence on the Explosion Mechanism and Metallicity, *Astrophys. J.* **749**, 91 (2012), [arXiv:1110.1726](https://arxiv.org/abs/1110.1726) [[astro-ph.SR](#)].
- [9] C. L. Fryer and V. Kalogera, Theoretical black hole mass distributions, *Astrophys. J.* **554**, 548 (2001), [arXiv:astro-ph/9911312](https://arxiv.org/abs/astro-ph/9911312).
- [10] M. Ugliano, H.-T. Janka, A. Marek, and A. Arcones, Progenitor-explosion Connection and Remnant Birth Masses for Neutrino-driven Supernovae of Iron-core Progenitors, *Astrophys. J.* **757**, 69 (2012), [arXiv:1205.3657](https://arxiv.org/abs/1205.3657) [[astro-ph.SR](#)].
- [11] T. Ertl, H.-T. Janka, S. E. Woosley, T. Sukhbold, and M. Ugliano, A Two-parameter Criterion for Classifying the Explodability of Massive Stars by the Neutrino-driven Mechanism, *Astrophys. J.* **818**, 124 (2016), [arXiv:1503.07522](https://arxiv.org/abs/1503.07522) [[astro-ph.SR](#)].
- [12] T. Sukhbold, T. Ertl, S. E. Woosley, J. M. Brown, and H.-T. Janka, Core-collapse Supernovae from 9 to 120 Solar Masses Based on Neutrino-powered Explosions, *Astrophys. J.* **821**, 38 (2016), [arXiv:1510.04643](https://arxiv.org/abs/1510.04643) [[astro-ph.HE](#)].
- [13] A. Burrows, D. Radice, and D. Vartanyan, Three-dimensional supernova explosion simulations of 9-, 10-, 11-, 12-, and 13- $M_{\odot}$  stars, *Mon. Not. Roy. Astron. Soc.* **485**, 3153 (2019), [arXiv:1902.00547](https://arxiv.org/abs/1902.00547) [[astro-ph.SR](#)].
- [14] L. Boccioli and G. Fragione, Remnant masses from 1  $D +$  core-collapse supernovae simulations: Bimodal neutron star mass distribution and black holes in the low-mass gap, *Phys. Rev. D* **110**, 023007 (2024), [arXiv:2404.05927](https://arxiv.org/abs/2404.05927) [[astro-ph.HE](#)].
- [15] C. S. Kochanek, J. F. Beacom, M. D. Kistler, J. L. Prieto, K. Z. Stanek, T. A. Thompson, and H. Yuksel, A Survey About Nothing: Monitoring a Million Supergiants for Failed Supernovae, *Astrophys. J.* **684**, 1336 (2008), [arXiv:0802.0456](https://arxiv.org/abs/0802.0456) [[astro-ph](#)].
- [16] C. S. Kochanek, Failed Supernovae Explain the Compact Remnant Mass Function, *Astrophys. J.* **785**, 28 (2014), [arXiv:1308.0013](https://arxiv.org/abs/1308.0013) [[astro-ph.HE](#)].
- [17] C. S. Kochanek, Constraints on Core Collapse from the Black Hole Mass Function, *Mon. Not. Roy. Astron. Soc.* **446**, 1213 (2015), [arXiv:1407.5622](https://arxiv.org/abs/1407.5622) [[astro-ph.SR](#)].
- [18] K. De *et al.*, Disappearance of a massive star in the Andromeda Galaxy due to formation of a black hole, *Science* **391**, adt4853 (2026), [arXiv:2410.14778](https://arxiv.org/abs/2410.14778) [[astro-ph.HE](#)].
- [19] C. S. Kochanek, J. M. M. Neustadt, and K. Z. Stanek, The Search for Failed Supernovae with the Large Binocular Telescope: The Mid-infrared Counterpart to N6946-BH1, *Astrophys. J.* **962**, 145 (2024), [arXiv:2310.01514](https://arxiv.org/abs/2310.01514) [[astro-ph.HE](#)].
- [20] S. M. Adams, C. S. Kochanek, J. R. Gerke, and K. Z. Stanek, The search for failed supernovae with the Large Binocular Telescope: constraints from 7 yr of data, *Mon. Not. Roy. Astron. Soc.* **469**, 1445 (2017), [arXiv:1610.02402](https://arxiv.org/abs/1610.02402) [[astro-ph.SR](#)].
- [21] R. Forés-Toribio and C. S. Kochanek, The neighboring stars of N6946-BH1 and the observational characteristics of failed supernovae, *arXiv* (2026), [arXiv:2604.05019](https://arxiv.org/abs/2604.05019) [[astro-ph.SR](#)].
- [22] S. Horiuchi, K. Nakamura, T. Takiwaki, K. Kotake, and M. Tanaka, The red supergiant and supernova rate problems: implications for core-collapse supernova physics, *Mon. Not. Roy. Astron. Soc.* **445**, L99 (2014), [arXiv:1409.0006](https://arxiv.org/abs/1409.0006) [[astro-ph.HE](#)].
- [23] K. Abe *et al.* (Super-Kamiokande), Diffuse supernova neutrino background search at Super-Kamiokande, *Phys. Rev. D* **104**, 122002 (2021), [arXiv:2109.11174](https://arxiv.org/abs/2109.11174) [[astro-ph.HE](#)].
- [24] K. Abe *et al.* (Super-Kamiokande), Search for Diffuse Supernova Neutrino Background with 956.2 days of Super-Kamiokande Gadolinium Dataset, *arXiv* (2025), [arXiv:2511.02222](https://arxiv.org/abs/2511.02222) [[astro-ph.HE](#)].
- [25] A. Lien, B. D. Fields, and J. F. Beacom, Synoptic Sky Surveys and the Diffuse Supernova Neutrino Background: Removing Astrophysical Uncertainties and Revealing Invisible Supernovae, *Phys. Rev. D* **81**, 083001 (2010), [arXiv:1001.3678](https://arxiv.org/abs/1001.3678) [[astro-ph.CO](#)].
- [26] P. Martínez-Miravé, I. Tamborra, M. Á. Aloy, and M. Obergaulinger, Diffuse neutrino background from magnetorotational stellar core collapses, *Phys. Rev. D* **110**,

- 103029 (2024), [arXiv:2409.09126 \[astro-ph.HE\]](#).
- [27] S. J. Smartt, Progenitors of Core-Collapse Supernovae, *Ann. Rev. Astron. Astrophys.* **47**, 63 (2009), [arXiv:0908.0700 \[astro-ph.SR\]](#).
- [28] B. Davies and E. R. Beasar, The ‘red supergiant problem’: the upper luminosity boundary of Type II supernova progenitors, *Mon. Not. Roy. Astron. Soc.* **493**, 468 (2020), [arXiv:2001.06020 \[astro-ph.SR\]](#).
- [29] S. Horiuchi, J. F. Beacom, C. S. Kochanek, J. L. Prieto, K. Z. Stanek, and T. A. Thompson, The Cosmic Core-collapse Supernova Rate does not match the Massive-Star Formation Rate, *Astrophys. J.* **738**, 154 (2011), [arXiv:1102.1977 \[astro-ph.CO\]](#).
- [30] W. M. Farr, N. Sravan, A. Cantrell, L. Kreidberg, C. D. Bailyn, I. Mandel, and V. Kalogera, The Mass Distribution of Stellar-Mass Black Holes, *Astrophys. J.* **741**, 103 (2011), [arXiv:1011.1459 \[astro-ph.GA\]](#).
- [31] F. Özel and P. Freire, Masses, Radii, and the Equation of State of Neutron Stars, *Ann. Rev. Astron. Astrophys.* **54**, 401 (2016), [arXiv:1603.02698 \[astro-ph.HE\]](#).
- [32] J. Antoniadis, T. M. Tauris, F. Özel, E. Barr, D. J. Champion, and P. C. C. Freire, The millisecond pulsar mass distribution: Evidence for bimodality and constraints on the maximum neutron star mass, [arXiv \(2016\)](#), [arXiv:1605.01665 \[astro-ph.HE\]](#).
- [33] J. Alsing, H. O. Silva, and E. Berti, Evidence for a maximum mass cut-off in the neutron star mass distribution and constraints on the equation of state, *Mon. Not. Roy. Astron. Soc.* **478**, 1377 (2018), [arXiv:1709.07889 \[astro-ph.HE\]](#).
- [34] Z.-Q. You *et al.*, Determination of the birth-mass function of neutron stars from observations, *Nature Astron.* **9**, 552 (2025), [arXiv:2412.05524 \[astro-ph.HE\]](#).
- [35] R. Abbott *et al.* (KAGRA, VIRGO, LIGO Scientific), GWTC-3: Compact Binary Coalescences Observed by LIGO and Virgo during the Second Part of the Third Observing Run, *Phys. Rev. X* **13**, 041039 (2023), [arXiv:2111.03606 \[gr-qc\]](#).
- [36] A. G. Abac *et al.* (LIGO Scientific, VIRGO, KAGRA), GWTC-4.0: Updating the Gravitational-Wave Transient Catalog with Observations from the First Part of the Fourth LIGO-Virgo-KAGRA Observing Run, [arXiv \(2025\)](#), [arXiv:2508.18082 \[gr-qc\]](#).
- [37] A. G. Abac *et al.* (LIGO Scientific, VIRGO, KAGRA), Searches for Binary Mergers with Sub-solar Mass Components in Data from the First Part of LIGO–Virgo–KAGRA’s Fourth Observing Run, [arXiv \(2026\)](#), [arXiv:2605.05444 \[astro-ph.HE\]](#).
- [38] B. Müller, T. M. Tauris, A. Heger, P. Banerjee, Y. Z. Qian, J. Powell, C. Chan, D. W. Gay, and N. Langer, Three-Dimensional Simulations of Neutrino-Driven Core-Collapse Supernovae from Low-Mass Single and Binary Star Progenitors, *Mon. Not. Roy. Astron. Soc.* **484**, 3307 (2019), [arXiv:1811.05483 \[astro-ph.SR\]](#).
- [39] A. Mezzacappa, E. Endeve, O. E. B. Messer, and S. W. Bruenn, Physical, numerical, and computational challenges of modeling neutrino transport in core-collapse supernovae, *Liv. Rev. Comput. Astrophys.* **6**, 4 (2020), [arXiv:2010.09013 \[astro-ph.HE\]](#).
- [40] H. Duan, G. M. Fuller, and Y.-Z. Qian, Collective Neutrino Oscillations, *Ann. Rev. Nucl. Part. Sci.* **60**, 569 (2010), [arXiv:1001.2799 \[hep-ph\]](#).
- [41] A. Mirizzi, I. Tamborra, H.-T. Janka, N. Saviano, K. Scholberg, R. Bollig, L. Hüdepohl, and S. Chakraborty, Supernova neutrinos: production, oscillations and detection, *Riv. Nuovo Cim.* **39**, 1 (2016), [arXiv:1508.00785 \[astro-ph.HE\]](#).
- [42] I. Tamborra and S. Shalgar, New Developments in Flavor Evolution of a Dense Neutrino Gas, *Ann. Rev. Nucl. Part. Sci.* **71**, 165 (2021), [arXiv:2011.01948 \[astro-ph.HE\]](#).
- [43] I. Tamborra, Neutrinos from explosive transients at the dawn of multi-messenger astronomy, *Nature Rev. Phys.* **7**, 285 (2025), [arXiv:2412.09699 \[astro-ph.HE\]](#).
- [44] M. C. Volpe, Neutrinos from dense environments: Flavor mechanisms, theoretical approaches, observations, and new directions, *Rev. Mod. Phys.* **96**, 025004 (2024), [arXiv:2301.11814 \[hep-ph\]](#).
- [45] L. Johns, S. Richers, and M.-R. Wu, Neutrino Oscillations in Core-Collapse Supernovae and Neutron Star Mergers, *Ann. Rev. Nucl. Part. Sci.* **75**, 399 (2025), [arXiv:2503.05959 \[astro-ph.HE\]](#).
- [46] B. Dasgupta, E. P. O’Connor, and C. D. Ott, Role of collective neutrino flavor oscillations in core-collapse supernova shock revival, *Phys. Rev. D* **85**, 065008 (2012), [arXiv:1106.1167 \[astro-ph.SR\]](#).
- [47] R. F. Sawyer, Speed-up of neutrino transformations in a supernova environment, *Phys. Rev. D* **72**, 045003 (2005), [arXiv:hep-ph/0503013 \[astro-ph\]](#).
- [48] R. F. Sawyer, Neutrino Cloud Instabilities Just above the Neutrino Sphere of a Supernova, *Phys. Rev. Lett.* **116**, 081101 (2016), [arXiv:1509.03323 \[astro-ph.HE\]](#).
- [49] S. Chakraborty, R. Hansen, I. Izaguirre, and G. G. Raffelt, Collective neutrino flavor conversion: Recent developments, *Nucl. Phys. B* **908**, 366 (2016), [arXiv:1602.02766 \[hep-ph\]](#).
- [50] I. Izaguirre, G. G. Raffelt, and I. Tamborra, Fast Pairwise Conversion of Supernova Neutrinos: A Dispersion Relation Approach, *Phys. Rev. Lett.* **118**, 021101 (2017), [arXiv:1610.01612 \[hep-ph\]](#).
- [51] S. Shalgar and I. Tamborra, Neutrino decoupling is altered by flavor conversion, *Phys. Rev. D* **108**, 043006 (2023), [arXiv:2206.00676 \[astro-ph.HE\]](#).
- [52] L. Johns, Collisional Flavor Instabilities of Supernova Neutrinos, *Phys. Rev. Lett.* **130**, 191001 (2023), [arXiv:2104.11369 \[hep-ph\]](#).
- [53] D. F. G. Fiorillo, H.-T. Janka, and G. G. Raffelt, Neutrino-Mass-Driven Instabilities as the Earliest Flavor Conversion in Supernovae, *Phys. Rev. Lett.* **135**, 231003 (2025), [arXiv:2507.22985 \[hep-ph\]](#).
- [54] J. Ehring, S. Abbar, H.-T. Janka, G. G. Raffelt, and I. Tamborra, Fast neutrino flavor conversion in core-collapse supernovae: A parametric study in 1d models, *Phys. Rev. D* **107**, 103034 (2023).
- [55] J. Ehring, S. Abbar, H.-T. Janka, and I. Raffelt, Georg G. and Tamborra, Fast Neutrino Flavor Conversions Can Help and Hinder Neutrino-Driven Explosions, *Phys. Rev. Lett.* **131**, 061401 (2023), [arXiv:2305.11207 \[astro-ph.HE\]](#).
- [56] H. Nagakura, Roles of Fast Neutrino-Flavor Conversion on the Neutrino-Heating Mechanism of Core-Collapse Supernova, *Phys. Rev. Lett.* **130**, 211401 (2023), [arXiv:2301.10785 \[astro-ph.HE\]](#).
- [57] T. Wang and A. Burrows, The Effect of the Fast-flavor Instability on Core-collapse Supernova Models, *Astrophys. J.* **986**, 153 (2025), [arXiv:2503.04896 \[astro-ph.HE\]](#).
- [58] R. Akaho, H. Nagakura, W. Iwakami, S. Furusawa, A. Harada, H. Okawa, H. Matsufuru, K. Sumiyoshi, and S. Yamada, Bifurcated Impact of Neutrino Fast Flavor

- Conversion on Core-Collapse Supernovae Informed by Multiangle Neutrino Radiation Hydrodynamics, *Phys. Rev. Lett.* **136**, 191002 (2026), arXiv:2601.08269 [astro-ph.HE].
- [59] K. Mori, T. Takiwaki, K. Kotake, and S. Horiuchi, Three-dimensional core-collapse supernova models with phenomenological treatment of neutrino flavor conversions, *Publ. Astron. Soc. Jap.* **77**, L9 (2025), arXiv:2501.15256 [astro-ph.HE].
- [60] M. Gogilashvili and I. Tamborra, Flavor Conversion Enhances or Suppresses Supernova Explodability Independent of the Progenitor Mass, in preparation (2026).
- [61] E. O'Connor and C. D. Ott, A new open-source code for spherically symmetric stellar collapse to neutron stars and black holes, *Class. Quant. Grav.* **27**, 114103 (2010), arXiv:0912.2393 [astro-ph.HE].
- [62] E. O'Connor, An Open-source Neutrino Radiation Hydrodynamics Code for Core-collapse Supernovae, *Astrophys. J. Supp.* **219**, 24 (2015), arXiv:1411.7058 [astro-ph.HE].
- [63] L. Boccioli, G. J. Mathews, and E. P. O'Connor, General Relativistic Neutrino-driven Turbulence in One-dimensional Core-collapse Supernovae, *Astrophys. J.* **912**, 29 (2021), arXiv:2102.06767 [astro-ph.HE].
- [64] S. M. Couch, M. L. Warren, and E. P. O'Connor, Simulating Turbulence-aided Neutrino-driven Core-collapse Supernova Explosions in One Dimension, *Astrophys. J.* **890**, 127 (2020), arXiv:1902.01340 [astro-ph.HE].
- [65] O. Just, S. Abbar, M.-R. Wu, I. Tamborra, H.-T. Janka, and F. Capozzi, Fast neutrino conversion in hydrodynamic simulations of neutrino-cooled accretion disks, *Phys. Rev. D* **105**, 083024 (2022), arXiv:2203.16559 [astro-ph.HE].
- [66] A. W. Steiner, M. Hempel, and T. Fischer, Core-collapse supernova equations of state based on neutron star observations, *Astrophys. J.* **774**, 17 (2013), arXiv:1207.2184 [astro-ph.SR].
- [67] K. Maltsev, F. R. N. Schneider, I. Mandel, B. Müller, A. Heger, F. K. Roepke, and E. Laplace, Explodability criteria for the neutrino-driven supernova mechanism, *Astron. Astrophys.* **700**, A20 (2025), arXiv:2503.23856 [astro-ph.SR].
- [68] E. E. Salpeter, The Luminosity function and stellar evolution, *Astrophys. J.* **121**, 161 (1955).
- [69] P. Kroupa, On the variation of the initial mass function, *Mon. Not. Roy. Astron. Soc.* **322**, 231 (2001), arXiv:astro-ph/0009005.
- [70] Z. Xiong and Y.-Z. Qian, Stationary solutions for fast flavor oscillations of a homogeneous dense neutrino gas, *Phys. Lett. B* **820**, 136550 (2021), arXiv:2104.05618 [astro-ph.HE].
- [71] I. Padilla-Gay, I. Tamborra, and G. G. Raffelt, Neutrino Flavor Pendulum Reloaded: The Case of Fast Pairwise Conversion, *Phys. Rev. Lett.* **128**, 121102 (2022), arXiv:2109.14627 [astro-ph.HE].
- [72] M. Zaizen and H. Nagakura, Simple method for determining asymptotic states of fast neutrino-flavor conversion, *Phys. Rev. D* **107**, 103022 (2023), arXiv:2211.09343 [astro-ph.HE].
- [73] M. Zaizen and H. Nagakura, Characterizing quasisteady states of fast neutrino-flavor conversion by stability and conservation laws, *Phys. Rev. D* **107**, 123021 (2023), arXiv:2304.05044 [astro-ph.HE].
- [74] H. Nagakura, L. Johns, and M. Zaizen, Bhatnagar-Gross-Krook subgrid model for neutrino quantum kinetics, *Phys. Rev. D* **109**, 083013 (2024), arXiv:2312.16285 [astro-ph.HE].
- [75] M. Goimil-García and I. Tamborra, Steady state of fast-oscillating neutrinos in an inhomogeneous medium, *Phys. Rev. D* **112**, 103011 (2025), arXiv:2509.22805 [astro-ph.HE].
- [76] J. Liu, H. Nagakura, M. Zaizen, L. Johns, and S. Yamada, Asymptotic states of fast neutrino-flavor conversions in the three-flavor framework, *Phys. Rev. D* **111**, 123004 (2025), arXiv:2503.18145 [astro-ph.HE].
- [77] Z. Xiong, M.-R. Wu, M. George, and C.-Y. Lin, Robust Integration of Fast Flavor Conversions in Classical Neutrino Transport, *Phys. Rev. Lett.* **134**, 051003 (2025), arXiv:2403.17269 [astro-ph.HE].
- [78] L. Johns, Subgrid modeling of neutrino oscillations in astrophysics, *Phys. Rev. D* **112**, 043024 (2025), arXiv:2401.15247 [astro-ph.HE].
- [79] H. Nagakura, General-relativistic quantum-kinetics neutrino transport, *Phys. Rev. D* **106**, 063011 (2022), arXiv:2206.04098 [astro-ph.HE].
- [80] S. Shalgar and I. Tamborra, Neutrino flavor conversion, advection, and collisions: Toward the full solution, *Phys. Rev. D* **107**, 063025 (2023), arXiv:2207.04058 [astro-ph.HE].
- [81] Z. Xiong, M.-R. Wu, M. George, C.-Y. Lin, N. Khosravi Largani, T. Fischer, and G. Martínez-Pinedo, Fast neutrino flavor conversions in a supernova: Emergence, evolution, and effects, *Phys. Rev. D* **109**, 123008 (2024), arXiv:2402.19252 [astro-ph.HE].
- [82] M. Cornelius, S. Shalgar, and I. Tamborra, Neutrino quantum kinetics in two spatial dimensions, *JCAP* **2024** (11), 060, arXiv:2407.04769 [astro-ph.HE].
- [83] S. Shalgar and I. Tamborra, Neutrino quantum kinetics in three flavors, *JCAP* **2025** (12), 026, arXiv:2503.03835 [astro-ph.HE].
- [84] E. Grohs, S. Richers, J. Froustey, F. Foucart, J. P. Kneller, and G. C. McLaughlin, Advection algorithms for quantum neutrino moment transport, *Phys. Rev. D* **111**, 083018 (2025), arXiv:2501.07540 [astro-ph.HE].
- [85] S. Richers, D. E. Willcox, N. M. Ford, and A. Myers, Particle-in-cell Simulation of the Neutrino Fast Flavor Instability, *Phys. Rev. D* **103**, 083013 (2021), arXiv:2101.02745 [astro-ph.HE].
- [86] J. Ehring, S. Abbar, H.-T. Janka, G. G. Raffelt, K. Nakamura, and K. Kotake, Gravitational-Wave Signatures of Nonstandard Neutrino Properties in Collapsing Stellar Cores, *Phys. Rev. Lett.* **136**, 021201 (2026), arXiv:2412.02750 [astro-ph.HE].
- [87] S. E. Woosley, A. Heger, and T. A. Weaver, The evolution and explosion of massive stars, *Rev. Mod. Phys.* **74**, 1015 (2002).
- [88] A. Chieffi and M. Limongi, The Presupernova Core Mass–Radius Relation of Massive Stars: Understanding Its Formation and Evolution, *Astrophys. J.* **890**, 43 (2020).
- [89] L. Boccioli, L. Roberti, M. Limongi, G. J. Mathews, and A. Chieffi, Explosion Mechanism of Core-collapse Supernovae: Role of the Si/Si-O Interface, *Astrophys. J.* **949**, 17 (2023), arXiv:2207.08361 [astro-ph.HE].
- [90] H.-T. Janka, Long-Term Multidimensional Models of Core-Collapse Supernovae: Progress and Challenges, *Ann. Rev. Nucl. Part. Sci.* **75**, 425 (2025), arXiv:2502.14836 [astro-ph.HE].
- [91] R. Bollig, N. Yadav, D. Kresse, H.-T. Janka, B. Müller, and A. Heger, Self-consistent 3D Supernova Models

- From  $-7$  Minutes to  $+7$  s: A 1-bethe Explosion of a  $\sim 19 M_{\odot}$  Progenitor, *Astrophys. J.* **915**, 28 (2021), [arXiv:2010.10506 \[astro-ph.HE\]](#).
- [92] E. E. Whitehead, R. Hirschi, V. Varma, B. Müller, F. Rizuti, C. Georgy, and W. D. Arnett, The impact of initial mass dependent convective boundary mixing on the structure and fates of massive stars, *Mon. Not. Roy. Astron. Soc.* **546**, staf2245 (2026), [arXiv:2512.11728 \[astro-ph.SR\]](#).
- [93] B. Müller, A. Heger, and J. Powell, Minimum Neutron Star Mass in Neutrino-Driven Supernova Explosions, *Phys. Rev. Lett.* **134**, 071403 (2025), [arXiv:2407.08407 \[astro-ph.HE\]](#).
- [94] Y. Kini *et al.*, A NICER View of PSR J0030+0451: Updated Constraints from Six Years of NICER Observations, *arXiv* (2026), [arXiv:2602.23743 \[astro-ph.HE\]](#).